

# Code modernization strategies for short-range non-bonded molecular dynamics simulations

James Vance<sup>1</sup>, Zhen-Hao Xu<sup>1</sup>, Nikita Tretyakov<sup>1</sup>, Torsten Stuehn<sup>2</sup>, Markus Rampp<sup>3</sup>, Sebastian Eibl<sup>3</sup>, André Brinkmann<sup>1</sup>

## Abstract

As modern HPC systems increasingly rely on greater core counts and wider vector registers, applications need to be adapted to fully utilize these hardware capabilities. One class of applications that can benefit from this increase in parallelism are molecular dynamics simulations. In this paper, we describe our efforts at modernizing the ESPResSo++ molecular dynamics simulation package by restructuring its particle data layout for efficient memory accesses and applying vectorization techniques to benefit the calculation of short-range non-bonded forces, which results in an overall three times speedup and serves as a baseline for further optimizations. We also implement finer-grain parallelism for multi-core CPUs through HPX, a C++ runtime system which uses lightweight threads and an asynchronous many-task approach to maximize parallelism. Our goal is to evaluate the performance of an HPX-based approach compared to the bulk-synchronous MPI-based implementation. This requires the introduction of an additional layer to the domain decomposition scheme that defines the task granularity. On spatially inhomogeneous systems, which impose a corresponding load-imbalance in traditional MPI-based approaches, we demonstrate that by choosing an optimal task size, the efficient work-stealing mechanisms of HPX can overcome the overhead of communication resulting in an overall 1.3 times speedup compared to the baseline MPI version.

## Keywords

molecular dynamics, high performance computing, HPX, MPI, ESPResSo++

## 1 Introduction

As the growth of processor frequency continues to plateau, modern HPC systems increasingly rely on greater concurrency and parallelism to deliver more floating-point performance. This comes in the form of increasing core counts and providing wider vector registers. However, as core counts increase, traditional parallelization methods that rely on MPI contend with fewer available memory per core and their performance faces increased sensitivity to load imbalances and synchronization mechanisms. Full utilization of wider vector registers also means critical parts of applications need to be rewritten and often requires more complex solutions. Thus, applications have to be adapted and modernized in order to fully maximize new hardware capabilities and overcome memory constraints.

Molecular dynamics (MD) simulations play a significant role in the study and discovery of new materials especially in soft matter research. They also act as an ideal example to harness more recent hardware capabilities since the calculations involved offer different ways of parallelization, such as through force decomposition, atom decomposition and spatial decomposition schemes (Plimpton 1995). Consequently, many simulation packages have been developed over the past decades that can run on machines with up to thousands and millions of cores such as LAMMPS (Plimpton 1995), GROMACS (Abraham et al. 2015) and NAMD (Phillips et al. 2020).

In this paper, we focus on ESPResSo++, an open-source software for performing molecular dynamics simulations of

condensed soft matter systems (Guzman et al. 2019). It is built on a C++ back-end with MPI-based communication enabling fast parallel execution. It also provides a Python frontend for convenient scripting and analysis. The foremost guideline in the design of ESPResSo++ is extensibility which allows it to become a sandbox in which users can easily develop new methods and algorithms (Halverson et al. 2013). However, this means that decisions taken to favor extensibility may not always result in the best optimized code for performance on modern hardware.

To address this, we investigate the use of SIMD vectorization and multithreaded task-based parallelism to improve the performance of ESPResSo++ on modern multi-core CPUs. We specifically focus on molecular dynamics simulations involving short-range non-bonded forces whose calculations take up a significant portion of the total simulation time and can benefit the most from these additional layers of parallelism.

<sup>1</sup>Zentrum für Datenverarbeitung, Johannes Gutenberg-Universität Mainz, Mainz, Germany

<sup>2</sup>Max Planck Institute for Polymer Research, Mainz, Germany

<sup>3</sup>Max Planck Computing and Data Facility, Garching, Germany

## Corresponding author:

James Vance, Zentrum für Datenverarbeitung, Johannes Gutenberg-Universität Mainz, Anselm-Franz-von-Bentzel-Weg 12, 55128 Mainz, Germany

Email: vance@uni-mainz.de

First, we maximize the utilization of wider vector registers through SIMD vectorization. SIMD, which stands for single instruction multiple data, allows a single instruction to simultaneously process multiple vector elements whose size depends on the bit length of registers known as the SIMD width (Watanabe and Nakagawa 2019). For example, Intel has been developing instruction set extensions over the years including Streaming SIMD Extensions (SSE) which support 128-bit registers, Advanced Vector Extensions (AVX) for 256-bit registers, and AVX-512 for 512-bit registers. These are often provided as functions called intrinsics which can be invoked directly from the source code but whose availability may vary among different architectures (Intel 2021b). To benefit from these extensions while retaining code portability, other approaches can be used such as directives that give the compiler hints about vectorizable loops (Intel 2021a) and libraries that implement generalized high-level abstractions to the underlying intrinsics such as the Vc library (Kretz and Lindenstruth 2012).

Next, we address the need for thread-level parallelism. Many applications that run on computing clusters, which includes ESPReso++, rely on the MPI programming paradigm which implicitly synchronizes calculation steps through communication. However, as the number of cores per node continues to increase, these applications become more sensitive to load imbalances and operating system noise causing wait times to increase. Such scenarios prevent good scaling of the application to large number of nodes unless a good load-balancing strategy is employed. An alternative approach to this is to use asynchronous many-task runtime systems which can handle increasing amounts of threads per node. One example is the Charm++ asynchronous programming model (Kale et al. 2021) on which the MD simulation package NAMD is built (Phillips et al. 2020). Another emerging candidate library is HPX, which is a C++ standards compliant library that provides wait-free asynchronous execution of tasks and synchronization through futures.

In this paper, we present our efforts at modernizing ESPReso++ by optimizing its data layout, enabling SIMD vectorization and integrating the capabilities for fine grain parallelism offered by HPX. Our aim is to evaluate the benefits of using HPX to provide node-level parallelism compared to traditional MPI-based parallelism.

This paper is structured as follows: In Section 2, we introduce some of the general concepts and calculations involved in molecular dynamics simulations and the particular design principles of ESPReso++. We also describe the details of the HPX library that are relevant to our work. In Section 3, we illustrate the serial optimizations we performed on the data layout and critical loops of ESPReso++ and show how we extended the pure MPI-based parallelization in ESPReso++ to an MPI+HPX parallelization model. Then, we evaluate the performance of these optimizations and show the results in Section 4. We list down related publications in Section 5. Finally, we conclude our work in Section 6 and discuss possible extensions to distributed parallelism in Section 7.

## 2 Background

In this section, we will recall the standard methods of performing molecular dynamics simulations on parallel machines. We will also discuss particular features and design principles of the target MD application, ESPReso++. Finally, we will introduce the asynchronous many-task programming paradigms that will be used in the parallel optimizations of ESPReso++.

### 2.1 Molecular dynamics simulations

Molecular dynamics (MD) simulations are used to model the dynamical properties of interacting particles in a system (Plimpton 1995; Leimkuhler and Matthews 2015). The central task of MD simulations is to integrate Newton's equations of motion

$$m_i \cdot \ddot{\mathbf{r}}_i = \mathbf{F}_i \quad (1)$$

where  $m_i$  is the mass of the particle  $i$ ,  $\mathbf{r}_i$  is its position vector and  $\mathbf{F}_i$  is the total force on  $i$  from interactions with all other particles in the simulation. Each of these forces can be derived from a potential energy  $U$  that depends on the coordinates of all  $N$  particles  $\mathbf{r}^N$  such that  $\mathbf{F} = -\nabla U$ . The forces may include pairwise interactions, three-body interactions and higher order many-body interactions.

The simulation evolves in an iterative process in which the positions are used to calculate the forces, which are in turn used to update the velocities and positions for the next time step. For the latter, known as the Integrate step, numerical integrators such as the velocity Verlet method are commonly employed (Verlet 1967; Swope et al. 1982).

#### 2.1.1 Short-range non-bonded potentials

Short-range force models comprise the most common class of interactions that are used in MD simulations. They physically result from electronic screening effects of long-range interactions and they also reduce computational load by restricting force contributions to a smaller region around each particle (Plimpton 1995).

One commonly used example is the Lennard-Jones (LJ) potential which is given by

$$V(r) = 4\varepsilon \left[ \left( \frac{\sigma}{r} \right)^{12} - \left( \frac{\sigma}{r} \right)^6 \right] \quad (2)$$

where  $\sigma$  and  $\varepsilon$  are parameters that describe the size of the particle and the depth of the potential well, respectively. Beyond some cutoff radius  $r_{\text{cut}}$  the interaction decays rapidly to zero. This means that to calculate the total force on one particle, the search for particle pairs can be confined to within a distance  $r < r_{\text{cut}}$  of the particle instead of the entire domain.

#### 2.1.2 Neighbor lists

Determining which particles are within cutoff of each other can be facilitated by binning the particles into rectangular cells of minimum length  $r_{\text{cut}}$ . Then the search for possible interaction pairs could be restricted to its cell and the 26 surrounding neighbor cells or 13 cells if the potential follows Newton's third law. The interacting particles may then be recorded in a list of pairs known as a Verlet list (Verlet 1967).

To reduce the computational cost of building the Verlet list, an additional buffer of thickness  $r_{\text{skin}}$  is introduced to the cell size such that  $r_{\text{cell}} \geq r_{\text{cut}} + r_{\text{skin}}$ . This allows some particles to move out of the neighborhood for some time steps without needing to reassign particles into cells and recompute the Verlet lists frequently.

### 2.1.3 Spatial decomposition

The most common way to parallelize molecular dynamics simulations on distributed-memory machines is by subdividing the simulation box into smaller *nodes*, each assigned to one processor (Plimpton 1995). Every processor takes care of computing the forces and updating positions and velocities of particles in its own node. Particles are then allowed to enter and exit a node by reassigning them to a different cell and subdomain during the resort step.

Each node is composed of *real cells* that belong to the spatial domain of that node and an outer layer of *ghost cells* that contain copies of particles from neighboring nodes (Halverson et al. 2013). The ghost cells are needed to correctly account for all force contributions at the subdomain boundaries and they are updated at each time step using local message-passing communication.

## 2.2 ESPResSo++

Started in 2008 as a joint collaboration between the Fraunhofer SCAI Institute and the Theory Group of the Max Planck Institute for Polymer Research, ESPResSo++ has become a central tool to perform coarse grained simulations and to provide a sophisticated and versatile framework for the development of new methods and algorithms. In order to simplify data exchange in complex workflows in combination with other software packages (e.g., LAMMPS, GROMACS, VOTCA), interfaces to these programs have been implemented. ESPResSo++ supports a variety of standard MD algorithms (e.g. Velocity-Verlet Integrator in NVE, NVT, NPT Ensembles) as well as several advanced methods (e.g. AdResS, H-AdResS, equilibration of polymer melts, Lattice Boltzmann, 3-body non-bonded Stillinger-Weber or the Tersoff potential) and modern data structures (e.g., H5MD) in parallel file I/O environments. More recent and ongoing developments include the integration of the ScaFaCoS library for long range interactions (Jülich Supercomputing Centre, 2014) and Lees-Edwards boundary conditions. Collaborative development within an international group of scientists, including continuous integration (CI) and Unit-Tests happens on the GitHub platform\*. ESPResSo++ is one of the central software packages of the Transregio SFB 146 and also part of the software pool of the European E-CAM project.

## 2.3 Asynchronous many-task programming models

Most applications that run on modern parallel architectures rely on the MPI+X programming model (Wolfe 2014) in which MPI handles inter-node communication and “X” is a hardware-dependent node-level programming paradigm such as OpenMP (OpenMP Architecture Review Board 2020), CUDA (NVIDIA 2021), or OpenACC (OpenACC-Standard.org 2020). An emerging class of new

parallel programming paradigms are asynchronous many-task (AMT) runtime systems which can provide fine-grain parallelism that can handle a large number of threads and efficiently distribute work across a node. One such example is HPX. The High Performance ParallelX (HPX) library is a C++ runtime system that can handle fine grain parallelism in modern architectures (Kaiser et al. 2020a). It allows users to write code based on a task dependency graph and takes care of the thread scheduling and execution of tasks and communication between distributed compute nodes.

We specifically focus on the thread management aspects of HPX to write and execute multithreaded code. This is achieved through the concept of *futurization*. HPX provides an asynchronous return type `hpx::future<T>` which hides the execution of function calls and returns immediately even though the function has not completed its execution. The futures can also be consumed by local control objects (LCOs) such as `hpx::future<T>::then`, `hpx::wait_all` and `hpx::shared_future`, which enable the flow of task dependencies. The API also provides high-level parallel algorithms aligned to current and future C++ standards and extends them with asynchronous versions (Kaiser et al. 2020a).

In the distributed case, HPX also provides an Active Global Address Space (AGAS) which registers objects with global identifiers that allows remote function calls while hiding explicit message passing. However, since we are focusing on node-level optimizations, AGAS will not be used in this work and inter-node communication will be done through MPI.

## 3 Optimizations

In this section, we discuss the key steps taken to improve the performance of ESPResSo++. We start with baseline optimizations that involve transforming the data layout and ensuring that use of SIMD vectorization is maximized by the compiler. Then, we implement thread-level parallelism by integrating the HPX runtime system into ESPResSo++.

The standard implementation of ESPResSo++ is heavily dependent on the Particle data structure. Since we want to maintain compatibility with the analysis tools in the current implementation while taking advantage of the performance improvements, we have chosen to implement the following optimizations as additional submodules within the `espressopp` Python module. The introduction of these submodules is facilitated by the extensibility and object-oriented design of ESPResSo++.

### 3.1 Improved data layout

Figure 1a shows the particle data layout in the standard implementation of ESPResSo++. All data for a single particle are stored in a large struct of 272 bytes called `Particle` including basic attributes such as type, position, velocity, force, and other attributes required for more complex simulations. The particles are further grouped into cells, each containing its own `std::vector<Particle>`. This layout was chosen since it provides the most straightforward

---

\*<https://www.github.com/espressopp>

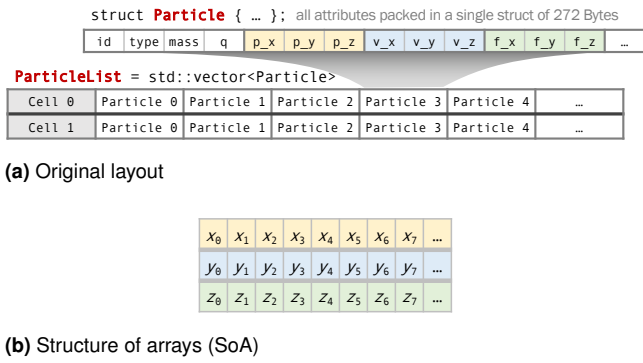


**Figure 1.** Original and improved layout for particle data

way of accessing particle data. This makes it compatible with the goal of extensibility and the object-oriented design of ESPResSo++, and it is well suited for algorithms working on nearly all particle data (Halverson et al. 2013). However, most of the time-consuming operations, such as force calculation and neighbor search, rely on only a few attributes. Performing those operations with this layout requires strided memory accesses through different attributes and operations with this layout cannot be vectorized.

In order to optimize these operations, we provide an alternative layout in the form of a structure of arrays (SoA) in which every attribute of type  $T$  is stored in its own separate `std::vector<T>` as shown in Figure 1b. SoA is known to improve cache re-use and allows for compiler-assisted vectorization of time-critical loops (Watanabe and Nakagawa 2019).

To maintain cache coherence and prevent false sharing during multi-threaded accesses, the member arrays are allocated aligned to 64-byte boundaries. For `std::vectors` this was done by using the `aligned_allocator` provided by the Boost.Align library<sup>†</sup>. The ends of cells are also padded with particles that lie far away from the simulation box to ensure that the entries for the next cell are also properly aligned.

The SoA layout is utilized only during the integrate and force calculation steps while the original layout is used in the resort stage since it requires all particle attributes. Thus, to ensure accuracy, the data between them are synchronized at the beginning and end of the simulation, and before and after the intermediate resort stages.

### 3.2 Vectorization

In this paper, we are specifically interested in optimizing for the vectorization capabilities provided by AVX-512 on Intel Skylake processors. However, we also want to keep critical loops portable to other compilers and CPU architectures while taking advantage of the SoA data layout. Thus, we mainly rely on compiler auto-vectorization to ensure that SIMD instructions are efficiently utilized. Additional directives were provided to inform the compiler of alignment and that there are no data dependencies among vector entries (Jeffers et al. 2016).

The most time-consuming sections of typical short-range non-bonded MD simulations are the neighbor list rebuild and the force calculation. Particularly for pair potentials, these steps require an efficient representation of the Verlet list. In

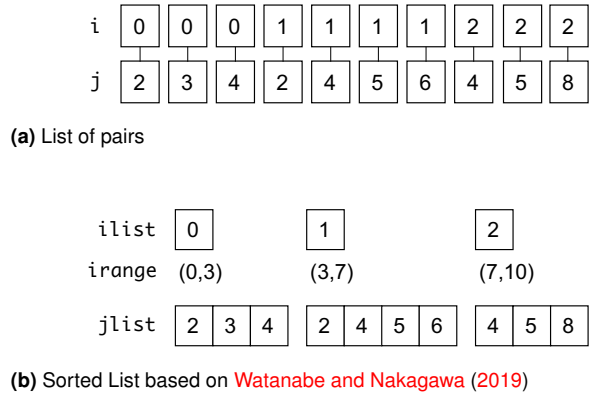


**Figure 2.** Possible representations of a Verlet list.

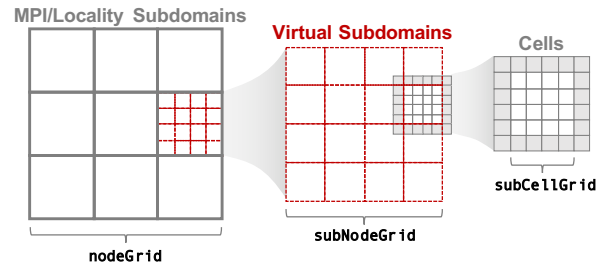


**Figure 3.** Dividing the MPI nodes further into subnodes which determine the task granularity.

the current version of ESPResSo++, it is represented as a list of pairs of pointers  $(i, j)$  to the corresponding `Particle` structs as shown in Figure 2a.

In our work, we use a more compact and vector-friendly representation known as a SORTEDLIST (Watanabe and Nakagawa 2019). Here the  $j$ -particles that interact with the same  $i$ -particle are grouped together and stored in a contiguous list as shown in Figure 2b. Thus, during force calculations the SORTEDLIST is traversed using a double for-loop: first, through the array of indices `ilist` and ranges `irange`, and then through the entries of `jlist` that are contained within the range. Since every  $i$  comes with distinct  $j$  entries, this structure leads to the possibility of applying vectorization on the inner for-loop over  $j$ .

### 3.3 Node-level parallelism using HPX

To enable multithreaded parallelism, we further divide the nodes into smaller *subnodes* as shown in Figure 3. Just like the MPI nodes, each subnode contains real cells belonging to that subnode's spatial domain and ghost cells from neighboring subnodes. This means that operations such as integration of positions and velocities, force calculation and Verlet list rebuilds can all be done in parallel for each subnode without needing explicit locking of resources. However, this new layer of decomposition introduces additional ghost cells that consume more memory and increases the communication overhead.

The number of cells within the subnode grid determines the task granularity. If the subnode is too small, execution

<sup>†</sup><https://www.boost.org/>



would be dominated by overheads. In contrast, a large grid size results in fewer subnodes to compute in parallel leading to resource starvation. Thus, the number of subnodes per core, known as an oversubscription factor, has to be tuned in order to find the optimal point between overheads and starvation (Bremer et al. 2019; Grubel et al. 2015). This auto-tuning procedure could be done by performing several runs of a few time-steps while varying the number of subnodes at each run, starting with the number of threads per MPI locality until no further decrease in elapsed time is recorded. This optimal number of subnodes will vary for every simulation system depending on the task size and relative load imbalances among the resulting subnodes with the assumption that the relative load distribution does not vary too much during the simulation.

To execute the MD operations in parallel across multiple threads, we rely on the C++ standards-compliant parallel algorithms provided by HPX. For the parallel execution of plain for-loops over subnodes we use `hpx::parallel::for_loop` and for operations involving reductions we use `hpx::parallel::transform_reduce`. Their signatures are similar to the C++ standard algorithms of the same name except that the first argument in HPX requires an executor which describes how to perform the algorithm in parallel. The adoption of executors has been planned for the C++23 standard, so that calls to functions in the `hpx` namespace can be replaced with `std` in the future.

Since the subnodes can be executed independently of each other after the ghost cells have been updated, the same functions for force calculation, neighbor list rebuilds and integration from the fully vectorized MPI version are used to implement the corresponding HPX versions of these functions. Thus, the limiting case of using one subnode per MPI node and one thread per MPI rank corresponds to the MPI version, which we use as baseline for our performance evaluation.

## 4 Performance evaluation

Evaluation was performed on the Mogon II supercomputer at the Johannes Gutenberg University Mainz using compute nodes equipped with two Intel Gold 6130 (Skylake) processors with a total of 32 cores per node running at 2.10 GHz base frequency and at least 96GB of memory. We used the following software versions: HWLOC 2.2.0, Boost 1.72.0, Python 3.8.2 and HPX 1.5.1 (Kaiser et al. 2020b). Binaries were compiled with Intel C++ Compiler 19.1 with the flags “-O3 -xHost -qopt-zmm-usage=high -restrict” to enable full AVX-512 optimizations.

Two simulation systems were used to evaluate performance – a Lennard-Jones simulation and a polymer melt simulation.

The Lennard-Jones simulation was initialized with particles in a cubic lattice at a density  $\rho = 0.8442$  and temperature  $T = 0.6$ . The parameters of the potentials in Equation (2) were set to  $\varepsilon = \sigma = 1$  with a cutoff distance  $r_{\text{cut}} = 2.5$  and a buffer thickness of  $r_{\text{skin}} = 0.3$ . A Langevin thermostat was introduced to equilibrate the particles to some temperature  $T$ .

We also prepared a polymer melt simulation containing ring polymers of chain length 200 and density  $\rho = 0.85$ . A repulsive Lennard-Jones interaction exists between all monomers within a cutoff distance  $r_{\text{cut}} = 2^{1/6}$  with parameters  $\varepsilon = \sigma = 1$  and skin size  $r_{\text{skin}} = 0.4$ . Aside from the short-range non-bonded interactions, the polymer melt simulation includes bonded interactions composed of a FENE potential between pairs along the chains and a cosine potential on triples that form angles (Kremer and Grest 1990).

The simulations were executed for a given number of time steps with a fixed step size  $\Delta t = 0.005$ . We measured the elapsed time of the integrator loop and excluded any initialization steps such as setting up classes and reading particle data. Within this period, the timings of the following key sections were also collected:

- Forces - calculating non-bonded (Lennard-Jones/Pair) and bonded (FENE, Angle) interactions
- Comm - communicating positions and collecting forces for ghost layers
- Integrate - updating positions and velocities
- Neigh - rebuilding neighbor lists
- Resort - sorting particles to cells and subdomains, and copying particle data between original and SoA layout

The values presented are averages across all MPI ranks.

### 4.1 Baseline optimizations

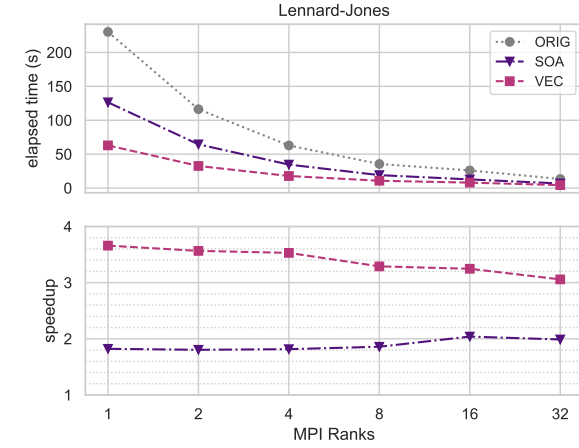
We first evaluated the performance benefits following the transformation of the particle data layout to SoA and the vectorization of critical loops. To do this, we compare three cases:

- ORIG - the original implementation,
- SOA - the implementation optimized with SoA particle data layout but with auto-vectorization disabled using the “-no-vec -no-simd” compiler flags, and
- VEC - the fully vectorized implementation.

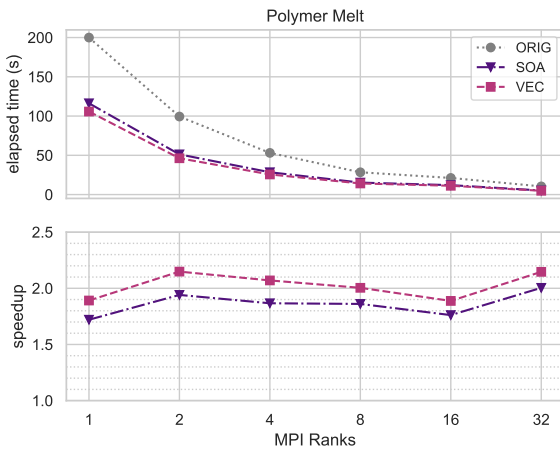
We performed the measurements on a single Skylake node using a Lennard-Jones fluid containing  $N = 262,144$  particles. The overall elapsed time and the speedup with respect to ORIG are shown in Figure 4a. On a full node, we observe a  $2\times$  speedup from ORIG to SOA due to the change in data layout, and a further  $1.5\times$  speedup from SOA to VEC due to the vectorization of the Lennard-Jones interaction and the neighbor list rebuild.

The elapsed time of different sections comparing runs on a full node are shown in Figure 4c. Speedups can be observed in all sections that use the SoA layout. However, there is an overhead in the resort section due to the additional copying of data from the SoA layout to the unoptimized layout on which the re-binning is performed. Among the different code sections, speedups resulting from vectorization are more significant in the force calculation and neighbor list rebuilds because these sections involve a traversal of the SORTEDLIST which has a higher trip count than the iteration through the particles in the other sections.

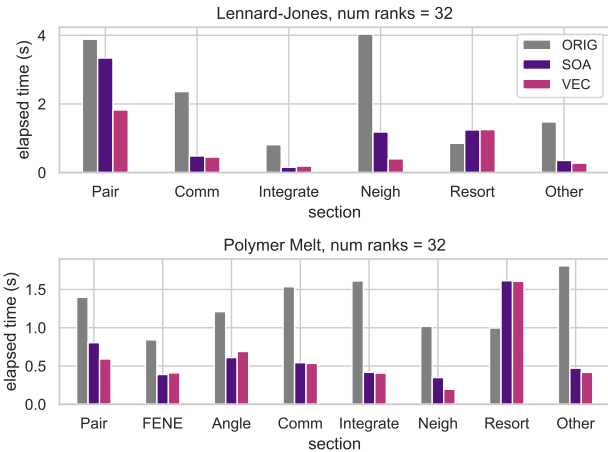
We also performed the same comparison on a polymer melt simulation with  $N = 320,000$  particles. As shown in Figure 4b, a similar  $2\times$  speedup is achieved from ORIG



(a) Lennard-Jones fluid



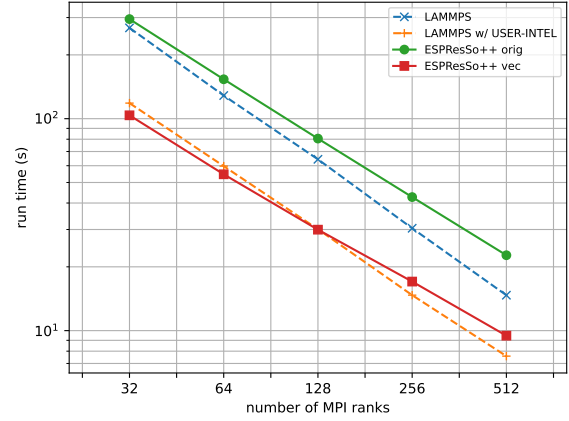
(b) Polymer melt



(c) Elapsed time for each code section at 32 ranks

**Figure 4.** Strong scaling. Speedups shown are calculated with respect to ORIG at the same number of MPI ranks.

to SOA. However, the speedup from SOA to VEC was reduced to only  $1.07\times$ . This is because the smaller cutoff for the Lennard-Jones potential results in fewer neighbors per particle at an average of 9.4 compared to 41.2 for the LJ setup, which in turn results in fewer iterations for the vectorized inner loop of the SORTEDLIST traversal in Pair and Neigh. Also, the other forces — FENE and Angle

**Figure 5.** Strong scaling comparison with LAMMPS

— were not vectorized in the same manner since they require mechanisms for conflict detection which are not yet supported by auto-vectorization.

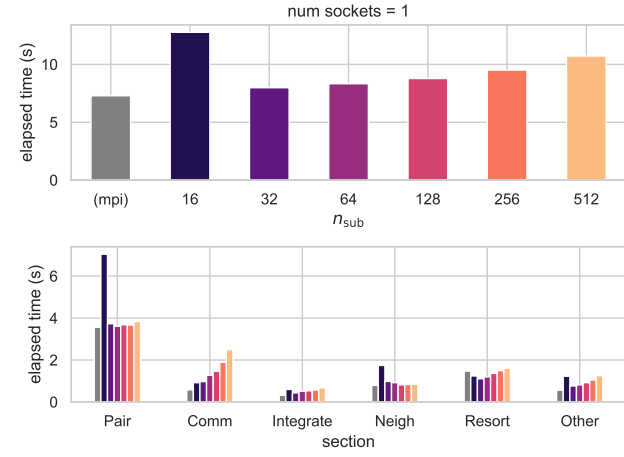
We also compare our vectorized implementation with LAMMPS which provides an Intel-optimized USER-INTEL package (Plimpton et al. 2020). We ran a strong scaling comparison against the original implementation and fully vectorized version of ESPResSo++ and present the results in Figure 5. We find a similar performance between LAMMPS USER-INTEL and the optimized version of ESPResSo++ with the latter having faster run time up to 128 MPI ranks. However, scalability is hindered by the resort stage which is still based on the original implementation and could be further improved in future implementations. Nevertheless, we have shown that even our serial optimizations already resulted in comparable parallel performance with LAMMPS.

## 4.2 MPI vs HPX comparison

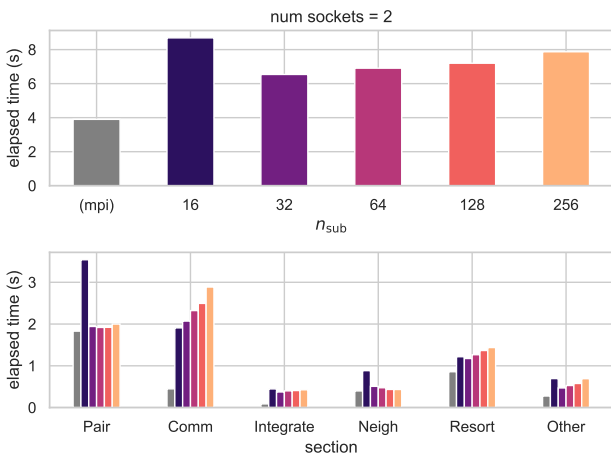
In this section, we evaluate our molecular dynamics implementation with HPX shared-memory parallelism in comparison to traditional MPI-based parallelism. We specifically investigate two cases: a spatially homogenous simulation to measure the overheads resulting from the HPX implementation, and a spatially inhomogeneous simulation to demonstrate load-balancing. In particular, we focus on single node performance since we want to investigate the benefits from the work-stealing capabilities of HPX. The MD simulations were executed on the same Skylake compute nodes equipped with two sockets each containing 16 cores, with one HPX thread assigned to each physical core.

We start with a spatially homogenous case in which we expect the simulation to be dominated by implementation overheads. We use the same Lennard-Jones setup from the previous section which contains  $N = 262,144$  particles and forms a cell grid of  $(24, 24, 24)$ . We perform the simulations for different numbers of subdomains per MPI rank,  $n_{\text{sub}}$ , starting from the number of cores on each socket and gradually increasing by a factor of two until no further subdivision is possible. This autotuning procedure allows us to find the optimal value of  $n_{\text{sub}}$ .

We first performed the evaluation for one MPI rank with 16 HPX threads on a single socket to isolate our



(a) Single socket case (16 cores, 1 MPI rank)



(b) Single node case (32 cores, 2 MPI ranks)

**Figure 6.** Elapsed time for the homogenous Lennard-Jones fluid with the MPI version and with HPX using different number of subnodes.

measurements from the effects of MPI communication. From the results shown in Figure 6a, an immediate drop in elapsed time can be seen from  $n_{\text{sub}} = 16$  to  $n_{\text{sub}} = 32$  followed by a steady slowdown as  $n_{\text{sub}}$  continues to increase. This means that executing two subdomains per thread is already sufficient since the pair force calculation does not improve anymore after this point. On the other hand, as  $n_{\text{sub}}$  increases, the number of ghost cells also increases resulting in a greater communication overhead. At the optimal point  $n_{\text{sub}} = 32$ , we find that the HPX implementation is 9% slower compared to the traditional MPI implementation where the overhead results from the too small task sizes at the integrate section.

The same simulation was then performed on two MPI ranks across two sockets with 16 HPX threads. From Figure 6b we see similar behavior except for a uniform increase in communication time. This results in a 40% slowdown compared to running one MPI task per core on the entire compute node. This is due to the fact that in the HPX implementation only the main thread in each MPI locality is performing communication so the number of communication

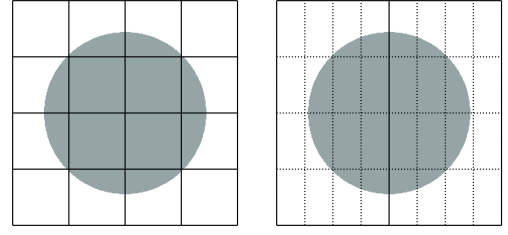


**Figure 7.** Initial spherical configuration of Lennard-Jones particles showing the domain decomposition at the  $x$ - $y$  plane with partitioning according to MPI ranks (—) and HPX subnodes (···). Left: MPI-only partitioning into (4, 4, 2) grid. Right: HPX-enabled partitioning into 2 MPI ranks and (4, 4, 4) subnode grid.

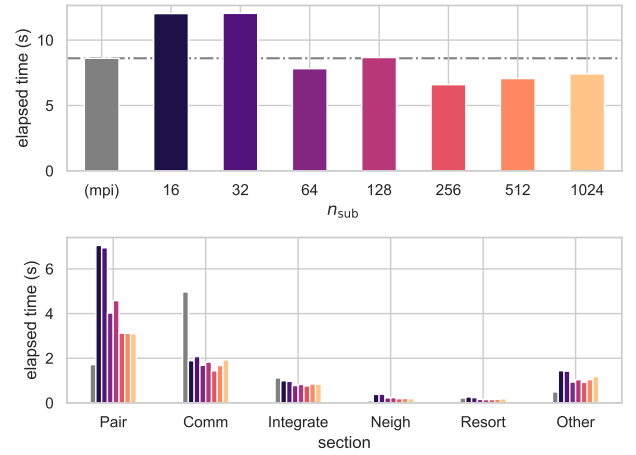


**Figure 8.** Comparison of section elapsed times for the spherical Lennard-Jones fluid

calls is reduced and the data volume for each call is increased.

To investigate a spatially inhomogeneous case, we construct a simulation using Lennard-Jones particles that mimics a spherical load distribution. This artificial setup replicates the load distribution arising in adaptive resolution simulations where particles in a spherical region are treated with full atomistic resolution, while the particles in the rest of the domain are coarse-grained resulting in reduced computational load. As shown in Figure 7, a spherical region in the center of a simulation box is filled with Lennard-Jones particles with density  $\rho_{\text{in}} = 0.8442$  similar to the bulk simulation described earlier. The portion of the simulation box outside of this sphere is also filled with particles with a different density  $\rho_{\text{out}} = \alpha \rho_{\text{in}}$  which is modulated through the density factor  $\alpha$ . For this setup, we use a larger cubic simulation box of length  $L = 271$  with a spherical region whose diameter occupies 70% of this length containing 2.58 million particles. To keep the spherical structure intact, the thermostat temperature was kept at  $T = 0.1$  and the simulation ran for 100 time steps.

Results of the autotuning procedure for a full compute node are shown in Figure 8. In contrast to the bulk simulation, the optimal number of subnodes for this setup has shifted to  $n_{\text{sub}} = 256$  with a  $1.3\times$  speedup over the MPI version. Among the different code sections, the

largest speedup can be observed in the communication which captures the MPI synchronization and takes the load imbalance into account. In the MPI version, the processors with fewer particles in their subdomain have to wait for other processors with more particles to complete their force calculations and synchronize via MPI. In the version with HPX multithreading, the work load is divided symmetrically between the two MPI ranks and the subnodes are executed concurrently by HPX threads.

## 5 Related work

Maximizing SIMD capabilities of recent hardware architectures has been thoroughly explored and applied to molecular dynamics simulations. For example, optimizations have been made in LAMMPS that enable full use of the Intel Knights Landing architecture with AVX-512 which is still relevant to more recent Intel CPUs (Jeffers et al. 2016). Watanabe and Nakagawa (2019) investigated SIMD vectorization techniques specifically for the Lennard-Jones potential on Intel CPUs with AVX2 and AVX-512 instructions.

Different forms of the hybrid MPI+X programming model have been widely applied in molecular dynamics simulations. For example, LAMMPS has OpenMP support for accelerators through CUDA and also provides a performance portable solution through Kokkos (Jeffers et al. 2016; Plimpton et al. 2020).

HPX has been successfully applied to N-body simulations of stellar mergers in astrophysics (Marcello et al. 2021). Grubel et al. (2015) studied the implication of task granularity on performance of HPX-based applications. Bremer et al. (2019) reported comparisons between the traditional MPI programming model and HPX-based implementations of the discontinuous Galerkin method for the two-dimensional shallow water equations.

## 6 Summary and discussion

In this work, we presented our code modernization efforts for the ESPReso++ molecular dynamics simulation package. This was achieved by optimizing the particle data layout, implementing SIMD vectorization on critical loops and integrating node-level parallelism through HPX. We have optimized operations that require only a few particle attributes by using a structure of arrays layout which improved the memory access patterns of these operations resulting in an up to  $2\times$  overall speedup. The change in layout also allowed us to ensure SIMD vectorization on critical for loops used in short-range interactions. This results in an additional  $1.5\times$  speedup for Lennard-Jones simulations and  $1.1\times$  speedup for polymer melt simulations, suggesting that the greater benefits from vectorization of short-range interactions depend on having a larger cut-off distance among other factors.

These serial optimizations served as a baseline on which we implemented node-level parallelism through HPX. By decomposing the MPI subdomain into smaller subnodes, we were able to modulate the granularity of the task sizes and obtain an optimum point between resource starvation and overhead from communicating ghost values between subnodes. We then compared the

HPX-based implementation with the traditional MPI-based parallelization. For a spatially homogenous system, we found the HPX implementation to be 9% slower on a single socket running a single MPI rank, which rises to 40% slower on a full node running two MPI ranks resulting from the increase in communication volume per MPI call. Nevertheless, the benefit of using the work-stealing capabilities of HPX was found when running spatially inhomogeneous simulations such as an LJ system with spherical load distribution for which we obtained a  $1.3\times$  speedup.

To maintain compatibility with the original packages within ESPReso++, we have chosen to implement our code modernization strategies as additional submodules in ESPReso++ (`vec` and `hpx4espp`). This is due to the intrusive change in the particle data structure which all algorithms and analysis tools are dependent on. This design choice allows us to continuously develop other performance improvements which could eventually be adopted in the main branch of ESPReso++.

Through this implementation and evaluation process, we have found that HPX can provide suitable features for implementing thread-level parallelism for MD applications involving short-range interactions while keeping MPI as the driver for inter-node communication. However, as with the introduction of any shared-memory programming model, certain care has to be taken in order to ensure thread-safety, which is not a concern in MPI-based implementations. We are able to solve this in our HPX implementation by introducing a node-level domain decomposition layer at the expense of additional communication overhead. By autotuning for a few time steps, we can find an optimal task size that maximizes parallelism and minimizes this overhead.

## 7 Future work

Further performance improvements can be achieved by utilizing HPX also for the distributed parallelism aspect of our application. The current implementation, which relies on the multithreaded parallel algorithms of HPX, is still limited by implicit synchronization among the different MPI localities since they still utilize MPI communication to update their ghost cells. This constraint can be further decoupled by allowing every subnode to independently perform ghost cell updates using asynchronous remote function calls. This can be done using the distributed parallelism framework of HPX through its Active Global Address Space (AGAS). Using global addressing, we can decouple the ghost communication among neighboring subnodes so that every direction can be updated independently through an API that is the same whether the neighboring subnode is in the same locality or not. This can then utilize the futurization capabilities of HPX to form a task-based dependency tree that will expose more parallelism and reduce the synchronization among MPI localities.

Although this work only addresses node-level load balancing through work-stealing, HPX can also be used to implement load balancing among different localities by converting the subnodes into migratable objects that can be moved between localities while maintaining their neighborhood topologies through their global addressability.



## Funding

This work was funded by the German Research Foundation (DFG) through the collaborative research center TRR 146 (Project G). Parts of this research were conducted using the supercomputer MOGON II and advisory services offered by Johannes Gutenberg University Mainz (hpc.uni-mainz.de), which is a member of the AHRP (Alliance for High Performance Computing in Rhineland Palatinate, [www.ahrp.info](http://www.ahrp.info)) and the Gauss Alliance.

## References

- Abraham MJ, Murtola T, Schulz R, Páll S, Smith JC, Hess B and Lindahl E (2015) GROMACS: High performance molecular simulations through multi-level parallelism from laptops to supercomputers. *SoftwareX* 1: 19–25. DOI:10.1016/j.softx.2015.06.001.
- Bremer M, Kazhyken K, Kaiser H, Michoski C and Dawson C (2019) Performance Comparison of HPX Versus Traditional Parallelization Strategies for the Discontinuous Galerkin Method. *Journal of Scientific Computing* 80(2): 878–902. DOI: 10.1007/s10915-019-00960-z.
- Grubel P, Kaiser H, Cook J and Serio A (2015) The Performance Implication of Task Size for Applications on the HPX Runtime System. *2015 IEEE International Conference on Cluster Computing* : 682–689 DOI:10.1109/cluster.2015.119. URL <http://stellar.cct.lsu.edu/pubs/hpcmaspa2015.pdf>.
- Guzman HV, Tretyakov N, Kobayashi H, Fogarty AC, Kreis K, Krajniak J, Junghans C, Kremer K and Stuehn T (2019) ESPReso++ 2.0: Advanced methods for multiscale molecular simulation. *Computer Physics Communications* 238: 66–76. DOI:10.1016/j.cpc.2018.12.017. URL <https://arxiv.org/pdf/1806.10841.pdf>.
- Halverson JD, Brandes T, Lenz O, Arnold A, Bevc S, Starchenko V, Kremer K, Stuehn T and Reith D (2013) ESPReso++: A modern multiscale simulation package for soft matter systems. *Computer Physics Communications* 184(4): 1129–1149. DOI: 10.1016/j.cpc.2012.12.004.
- Intel (2021a) Intel® C++ Compiler Classic Developer Guide and Reference. URL [https://software.intel.com/content/dam/develop/external/us/en/documents/cpp\\_compiler\\_classic.pdf](https://software.intel.com/content/dam/develop/external/us/en/documents/cpp_compiler_classic.pdf).
- Intel (2021b) Intel® Intrinsics Guide. URL <https://software.intel.com/sites/landingpage/IntrinsicsGuide>.
- Jeffers, Reinders, James and, Sodani, James and and Avinash (2016) *Intel Xeon Phi processor high performance programming: knights landing edition*. Morgan Kaufmann. ISBN 978-0128091944. URL <https://dl.acm.org/doi/10.5555/3050856>.
- Kaiser H, Diehl P, Lemoine A, Leibach B, Amini P, Berge A, Biddiscombe J, Brandt S, Gupta N, Heller T, Huck K, Khatami Z, Kheirkhahan A, Reverdel A, Shirzad S, Simberg M, Wagle B, Wei W and Zhang T (2020a) HPX - The C++ Standard Library for Parallelism and Concurrency. *Journal of Open Source Software* 5(53): 2352. DOI:10.21105/joss.02352.
- Kaiser H et al. (2020b) STELLAR-GROUP/hpx: HPX V1.5.1: The C++ Standards Library for Parallelism and Concurrency. DOI: 10.5281/zenodo.4059746. URL <https://doi.org/10.5281/zenodo.4059746>.
- Kale L et al. (2021) Uiuc-ppl/charm: v7.0.0-rc1. DOI:10.5281/zenodo.4988098. URL <https://doi.org/10.5281/zenodo.4988098>.
- Kremer K and Grest GS (1990) Dynamics of entangled linear polymer melts: A molecular-dynamics simulation. *The Journal of Chemical Physics* 92(8): 5057–5086. DOI:10.1063/1.458541.
- Kretz M and Lindenstruth V (2012) Vc: A C++ library for explicit vectorization. *Software: Practice and Experience* 42(11): 1409–1430. DOI:10.1002/spe.1149.
- Leimkuhler B and Matthews C (2015) *Molecular Dynamics, With Deterministic and Stochastic Numerical Methods*. Interdisciplinary Applied Mathematics. Springer. ISBN 9783319163741. DOI:10.1007/978-3-319-16375-8.
- Marcello DC, Shiber S, De Marco O, Frank J, Clayton GC, Motl PM, Diehl P and Kaiser H (2021) Octo-tiger: a new, 3d hydrodynamic code for stellar mergers that uses hpx parallelization. *Monthly Notices of the Royal Astronomical Society* 504(4): 5345–5382.
- NVIDIA (2021) CUDA Toolkit v11.4.2. URL <https://developer.nvidia.com/cuda-toolkit>.
- OpenACC-Standardorg (2020) The OpenACC Application Programming Interface (version 3.1). URL <https://www.openacc.org/sites/default/files/inline-images/Specification/OpenACC-3.1-final.pdf>.
- OpenMP Architecture Review Board (2020) OpenMP application programming interface (version 5.1). URL <https://www.openmp.org/spec-html/5.1/openmp.html>.
- Phillips JC, Hardy DJ, Maia JDC, Stone JE, Ribeiro JV, Bernardi RC, Buch R, Fiorin G, Hénin J, Jiang W, McGreevy R, Melo MCR, Radak BK, Skeel RD, Singharoy A, Wang Y, Roux B, Aksimentiev A, Luthey-Schulten Z, Kalé LV, Schulten K, Chipot C and Tajkhorshid E (2020) Scalable molecular dynamics on CPU and GPU architectures with NAMD. *The Journal of Chemical Physics* 153(4): 044130. DOI:10.1063/5.0014475.
- Plimpton S (1995) Fast Parallel Algorithms for Short-Range Molecular Dynamics. *Journal of Computational Physics* 117(1): 1–19. DOI:10.1006/jcph.1995.1039.
- Plimpton S, Kohlmeyer A, Thompson A, Moore S and Berger R (2020) LAMMPS Stable release 29 October 2020. DOI: 10.5281/zenodo.4157471. URL <https://doi.org/10.5281/zenodo.4157471>.
- Swope WC, Andersen HC, Berens PH and Wilson KR (1982) A computer simulation method for the calculation of equilibrium constants for the formation of physical clusters of molecules: Application to small water clusters. *The Journal of Chemical Physics* 76(1): 637–649. DOI:10.1063/1.442716.
- Verlet L (1967) Computer "Experiments" on Classical Fluids. I. Thermodynamical Properties of Lennard-Jones Molecules. *Physical Review* 159(1): 98–103. DOI:10.1103/physrev.159.98.
- Watanabe H and Nakagawa KM (2019) SIMD vectorization for the Lennard-Jones potential with AVX2 and AVX-512 instructions. *Computer Physics Communications* 237: 1–7. DOI:10.1016/j.cpc.2018.10.028. URL <https://doi.org/10.1016/j.cpc.2018.10.028>.
- Wolfe M (2014) Compilers and more: MPI+ X. *HPC Wire* .